

## Article

# Characterizing Changes in Streamflow and Sediment Supply in the Sacramento River Basin, California, Using Hydrological Simulation Program—FORTRAN (HSPF)

Michelle Stern <sup>1,\*</sup>, Lorraine Flint <sup>1</sup>, Justin Minear <sup>2</sup>, Alan Flint <sup>1</sup> and Scott Wright <sup>1</sup>

<sup>1</sup> California Water Science Center, United States Geological Survey, Sacramento, CA 95819, USA; lflint@usgs.gov (L.F.); aflint@usgs.gov (A.F.); sawright@usgs.gov (S.W.)

<sup>2</sup> Geomorphology and Sediment Transport Laboratory, United States Geological Survey, Golden, CO 80403, USA; jminear@usgs.gov

\* Correspondence: mstern@usgs.gov; Tel.: +1-916-278-3093

Academic Editor: Xuan Yu

Received: 14 May 2016; Accepted: 19 September 2016; Published: 30 September 2016

**Abstract:** A daily watershed model of the Sacramento River Basin of northern California was developed to simulate streamflow and suspended sediment transport to the San Francisco Bay-Delta. To compensate for sparse data, a unique combination of model inputs was developed, including meteorological variables, potential evapotranspiration, and parameters defining hydraulic geometry. A slight decreasing trend of sediment loads and concentrations was statistically significant in the lowest 50% of flows, supporting the observed historical sediment decline. Historical changes in climate, including seasonality and decline of snowpack, contribute to changes in streamflow, and are a significant component describing the mechanisms responsible for the decline in sediment. Several wet and dry hypothetical climate change scenarios with temperature changes of 1.5 °C and 4.5 °C were applied to the base historical conditions to assess the model sensitivity of streamflow and sediment to changes in climate. Of the scenarios evaluated, sediment discharge for the Sacramento River Basin increased the most with increased storm magnitude and frequency and decreased the most with increases in air temperature, regardless of changes in precipitation. The model will be used to develop projections of potential hydrologic and sediment trends to the Bay-Delta in response to potential future climate scenarios, which will help assess the hydrological and ecological health of the Bay-Delta into the next century.

**Keywords:** HSPF; watershed hydrology; suspended sediment; hydrologic modeling; water resources; San Francisco Bay-Delta; Sacramento River; sediment transport

## 1. Introduction

The Sacramento River Basin of northern California (Figure 1) produces 84% of the fresh water inflow and 80% of the sediment to the San Francisco Bay-Delta (Bay-Delta) [1]. The Computational Assessments of Scenarios of Change for the Delta Ecosystem (CASCaDE II) project [2] is developing a better understanding of how potential future changes in the characteristics and climate of watersheds draining into the Bay-Delta will affect water quality, ecosystem processes, and critical species. Turbidity, geomorphic change, and wetland stability all depend on sediment supply; therefore, sediment supply has critical implications for the ecology of the Bay-Delta [3]. The total sediment load has decreased by 50% during the last 50 years for a suite of interacting reasons, including the diminishment of the sediment pulse created during 19th century hydraulic mining in the Sierra Nevada, sediment trapping behind reservoirs, deposition of sediment in flood bypasses, and armoring of river channels [4].

Turbidity is related to sediment and therefore a decline in sediment supply contributes to undesirable conditions for key fish species such as the delta smelt [5]. Discharge from the Sacramento River is a primary driver of turbidity in critical delta smelt habitat and thus has implications for the future survival of delta smelt and other species which share similar ecological preferences [5].

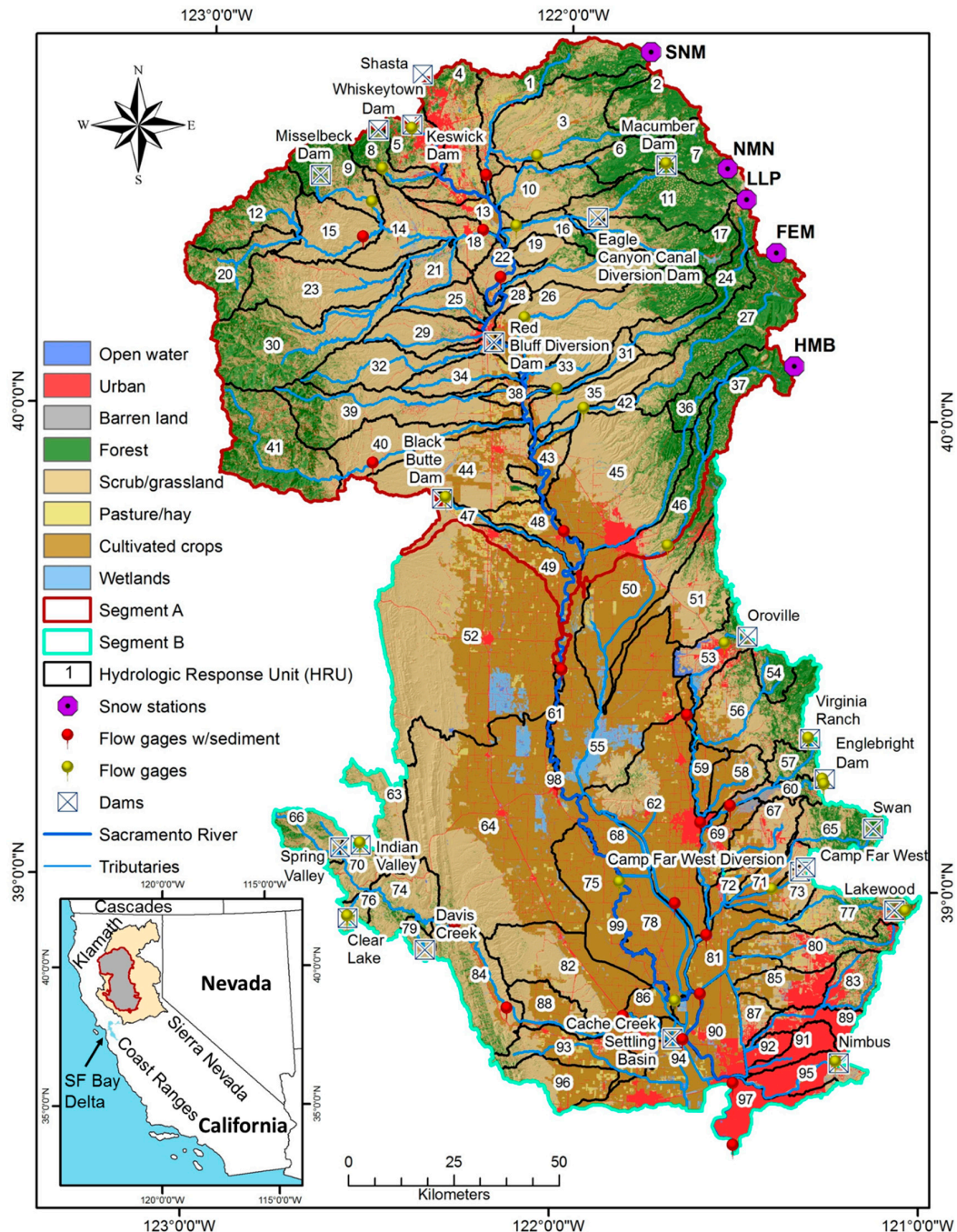


**Figure 1.** Location map of the Sacramento River Basin model domain, CA, indicating: land use, snow stations, major California dams/diversions, hydrologic and sediment gages, and model reaches. Total drainage area of the Sacramento River is indicated (orange of inset). California Data Exchange Center (CDEC) snow stations are abbreviated as: SNM = Snow Mountain; NMN = New Manzanita Lake; LLP = Lower Lassen Peak; FEM = Feather River Meadow; HMB = Humbug. Inset indicates major mountain ranges, and Sacramento Valley surface water drainage in orange, and model domain in gray.

The main objective of this project was to develop a spatially distributed daily streamflow and sediment transport model of the Sacramento River Basin to link with a hydrodynamic model of the Bay-Delta, and to characterize the changes in sediment transport over the historical record. The Sacramento River Basin supplies the majority of the sediment to the Bay-Delta, and representing the mechanisms of sediment transport in the watershed is important to assess the impact of potential changes in future climate regimes. Because of limited measured suspended sediment data, the model was calibrated to available data below major dams and impoundments, and will be used to simulate potential future changes in sediment delivery to the Bay-Delta under climate change. The approach of this study relied on the development of a unique combination of spatially distributed climate variables and hydraulic function tables, and the preservation of spatially distributed information during calibration. This allowed for the extrapolation of known processes to areas without calibration data, resulting in a robust calibration. This approach is generally in contrast with typical methods used in large river basins that depend on one to a few climate stations, sometimes without interpolation across the watershed, and individual calibration of hydrologic response units without consideration of distributed properties across the landscape.

The current conceptual model of sediment decline in the Sacramento River basin [6] attributes hydraulic mining and dams and reservoirs as the likely anthropogenic causes, and relies on qualitative descriptions of sediment drivers and linkages, in addition to a water and sediment budget using four years of data. The development of this model has allowed us to investigate the role of climate on sediment transport in this basin, and how changes in climate over the last 50 years have contributed to changes in sediment delivery to the Bay-Delta.

### *Study Area*

The Sacramento River drainage is being studied because of its dominant contribution of sediment supply to the Bay-Delta. It is a  $6.8 \times 10^4$  km<sup>2</sup> area in the northern part of the Central Valley of California (Figure 1, inset) and it comprises over half of the total drainage area of the Bay-Delta [7]. The Sacramento River is the longest river system in the state of California, and it is a complex and highly managed system. Dams located in the foothills surrounding the valley floor restrict flow in most of the tributaries to the main stem of the Sacramento River. The majority of floodwater in the lower Sacramento River is diverted using a series of passive weirs into a system of flood bypasses, which act as natural conveyance floodplains by transferring excess streamflow directly into the Bay-Delta [8]. The weir and bypass system was built before most of the large dams were constructed in 1920–1970. The dams were installed to assist in flood control, for power generation, and to provide water for downstream use, with ~38% used for agricultural irrigation, and ~4% for urban use [9]. Reservoirs behind the dams have accumulated large amounts of sediment and gravels as a byproduct of hydraulic mining in the late 19th century, in addition to land use changes within the watershed [6]. The study area within the Sacramento River Basin has an area of roughly 26,000 km<sup>2</sup>, and begins below Keswick Dam (Figure 1). The largest contribution of flow to the Sacramento River in the model domain is the outflow from Keswick Dam, which is fed by the outflow from Shasta Dam nearly 16 km upstream from Keswick Dam (Figure 1).

## **2. Methods**

The methods described below focus on non-standard methods and approaches used to develop this model. Standard Hydrological Simulation Program—FORTRAN (HSPF) methods used are described in the Supplementary Materials (S1–S5).

### *2.1. Hydrological Simulation Program—FORTRAN (HSPF)*

A watershed model for the Sacramento River Basin was developed to simulate streamflow and suspended sediment for the period 1958–2008 using the Hydrological Simulation Program—FORTRAN (HSPF) [10]. HSPF was chosen for this study because it is a comprehensive process-based watershed

model that can be used to simulate daily streamflow and suspended sediment for a continuous multi-year period and for a wide range of watershed sizes and conditions [11]. HSPF is useful for modeling natural and developed watersheds, and is effective for land surface and subsurface hydrology as well as water quality processes. Importantly, it enables the user to create alternative scenarios by adjusting land use or meteorological variables such as air temperature or precipitation [11].

HSPF is a spatially distributed and temporally continuous simulation model that employs lumped parameter segments. Each sub-watershed or hydrologic response unit (HRU) is considered homogeneous with the same set of parameters. Three modules in the HSPF model represent the major watershed processes. Pervious land is modeled in the PERLND module, impervious land in the IMPLND module, and the RCHRES module simulates the processes in streams or reservoirs. A comprehensive functional description of HSPF can be found in Bicknell et al., 2001 [10]. In this paper, the segments from the combined PERLND and IMPLND modules will be referred to as hydrologic response units or HRUs, and RCHRES will be referred to as reaches. Sediment sources are modeled in HSPF as wash-off detached sediment in surface storage and scour of the soil matrix of PERLNDs, and as bedload scour in RCHRESs. Sediment transport is modeled as an advective, non-reactive constituent of streamflow, with deposition and scour dependent on the simulated flow velocity and particle size of the sediment. Bedload and suspended sediment are simulated as separate components; however, longitudinal bedload transport is not simulated in HSPF.

The HSPF model was developed for the Sacramento River Basin at a daily time step to simulate streamflow and suspended sediment concentrations (SSC) in the Sacramento River and tributaries below major dams. HSPF allows for daily, hourly, and sub-hourly time intervals; however, meteorological data within the model domain were not widely available at hourly or sub-hourly time increments, and therefore a daily time step was considered appropriate for the purposes of this study.

## 2.2. HSPF Input

Data used to develop the HSPF model included: the 2006 land use data from the National Land Cover Database (NLCD) ([mrlc.gov/nlcd2006.php](http://mrlc.gov/nlcd2006.php)) [12], elevation data from the National Elevation Dataset (NED) ([ned.usgs.gov/](http://ned.usgs.gov/)) [13], and the hydrology and stream network from the USGS National Hydrography Dataset (NHD) ([nhd.usgs.gov/](http://nhd.usgs.gov/)) [14]. Soils data were obtained from the Soil Survey Geographic (SSURGO) [15] database, including erosion potential (k-factor), texture (percent sand silt and clay), hydrologic soil group, available water storage capacity, and surface texture. Time series data including meteorological station data, streamflow, dam releases, snow water equivalent, and suspended sediment and sediment loads were collected for the time period 1958–2008. Station data for the meteorological development (air temperature, precipitation, and solar radiation) were collected from the National Weather Service (NWS) Cooperative Observer Program (COOP, [www.ncdc.noaa.gov/](http://www.ncdc.noaa.gov/)), Remote Automated Weather Stations (RAWS, [www.raaws.dri.edu/](http://www.raaws.dri.edu/)), and California Irrigation Management Information System (CIMIS, [www.cimis.water.ca.gov/](http://www.cimis.water.ca.gov/)) stations within the study area. Solar radiation, wind speed, cloud cover and dew point were downloaded from the Fair Oaks CIMIS station. Streamflow, snow and sediment calibration and boundary condition data are described in the Supplementary Materials (S1), the development of boundary dam conditions is described in S2, and the development of hydrologic response units in S3.

### 2.2.1. Gridded Meteorological Inputs to HSPF

HSPF does a reasonable job of predicting hydrology, sediment, water quality, and pollutant loads; however, the inability of meteorological stations to cover the spatial variations of precipitation and the uncertainty of managed flow data (diversions and return flows) are major limiting factors of more accurate predictions [16]. A better spatial representation of watershed precipitation was found to improve model accuracy, even for a semi-lumped model [17]. HSPF typically assigns data from meteorological stations directly to each sub-basin using Thiessen polygons. Meteorological stations are sparsely located in some areas and are not all active on any given day. Typical HSPF models rely on very



few climate stations, some with only one station to represent the entire watershed [18–21]. The objective of the meteorological development was to enhance the spatial distribution of daily meteorological data and therefore increase the accuracy of modeled streamflow and suspended sediment. Incorporating gridded meteorological data as an input to HSPF has been successfully demonstrated [17,22] and, as the key driver of the rainfall runoff process and sediment transport, was shown to have increased the accuracy of the hydrologic results [17].

Meteorological data from climate stations consisting of daily precipitation and air temperature were spatially interpolated over the model domain using the Gradient Inverse Distance Squared (GIDS) spatial interpolation [23]. Spatial interpolation of meteorological data can be inaccurate when there are few stations and large distances between stations. The GIDS method provides accuracies at least as good as established kriging techniques without the complexity and subjectivity of kriging and the required station density [23,24]. For every active station, GIDS develops regressions for each day including the variables northing, easting, and elevation to interpolate to each grid cell, in this case, 270 m. This approach provides a detailed and localized incorporation of topographic and regional influences on precipitation (Figure 2A).

Precipitation was summed and the temperature was averaged to transform the daily maps into monthly maps. PRISM data (Parameter-elevation Regressions on Independent Slopes Model) ([prism.oregonstate.edu/](http://prism.oregonstate.edu/)) (Figure 2B) are recognized as high-quality spatial climate data sets [25] and were spatially downscaled using GIDS to the 270 m scale and used for comparison to match the measured data trend and to keep the regional monthly spatial structures intact. A ratio was developed for each grid cell using monthly PRISM values. The daily GIDS maps were multiplied by the PRISM ratio to produce daily meteorological values (Figure 2C) that sum or average to exactly match PRISM monthly values. This method was applied to precipitation and air temperature data, and the data were spatially distributed to each HRU (Figure 2D). This method is an improvement on the typical distribution of meteorological stations because the measured data spatial trend is preserved and the regional monthly structures are incorporated across the watershed to produce better interpolations when data stations are not present for any given day.

Potential evapotranspiration (PET) is an important component of the water balance equation in HSPF. PET can be estimated directly by HSPF or estimated using pre-processing methods and applied as a daily time series for each HRU and reach. For this project, estimates of daily PET were developed as a pre-processing step using the Priestley-Taylor equation [26], simulated hourly solar radiation, including topographic shading and atmospheric parameters, estimated cloudiness, and the gridded daily air temperature estimates described above. Cloudiness was estimated using the Bristow-Campbell equation [27] which was calibrated to CIMIS and RAWS daily measured solar radiation and the gridded air temperature data. This method of estimating PET is considered to be an improvement over internal HSPF calculations that use pan-evaporation measurements with an adjustment factor or other temperature-based equations to distribute PET to each HRU. The Priestley-Taylor equation is an energy balance equation that has a non-linear relationship of PET to temperature that is considered more appropriate when extrapolating PET into the future when elevated air temperatures are projected to persist [28]. Other formulas that use a linear relationship of PET to air temperature have been shown to overestimate PET under warming climates [28]. The PET estimates using the Priestley-Taylor equation were calibrated to all California Irrigation Management Information System (CIMIS) stations in the study area and then distributed as a daily time series to each HRU.

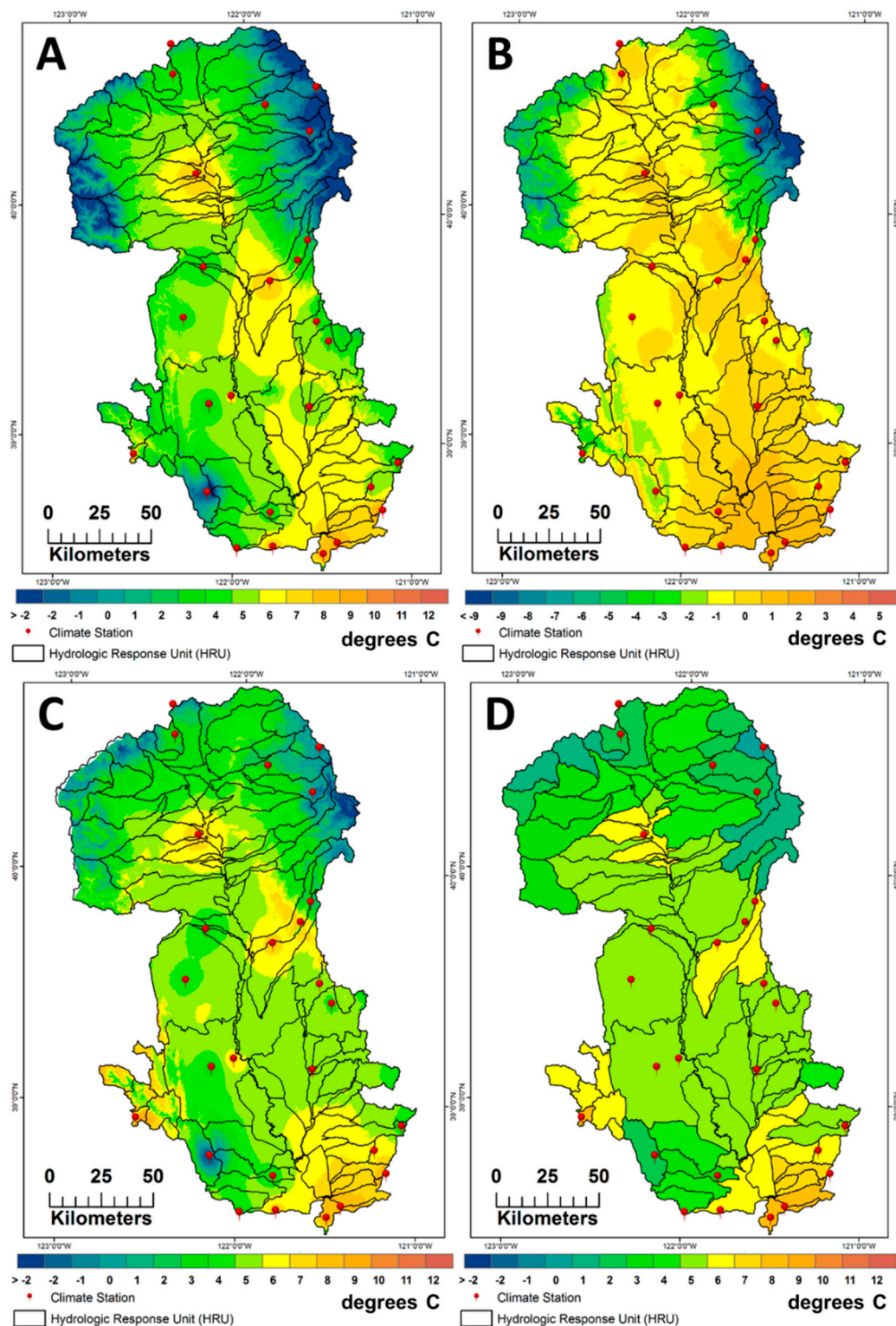


**Figure 2.** Example of meteorological development (minimum air temperature) for 12 January 1957 using the GIDS (Gradient Inverse Distance Squared) interpolation and PRISM (Parameter-elevation Regressions on Independent Slopes Model) data. Of 78 available stations within the region, 42 were active on this day and used in the development, and 26 are shown above within the study area boundary. The development includes (A) GIDS-developed regressions for each day including the variables northing, easting, and elevation to interpolate to each 270 m grid cell; (B) PRISM monthly map used to create a ratio for scaling maps of daily interpolated station data; (C) daily GIDS maps multiplied by the PRISM ratio to produce daily meteorological values that sum or average to exactly match PRISM monthly values; and (D) scaled daily data for each hydrologic response unit that were averaged for model input.

### 2.2.2. FTABLE Development

HSPF uses a hydraulic function table (FTABLE) to represent the geometric and hydraulic properties of stream reaches and reservoirs [29]. FTABLEs define the stage-area-volume-discharge relation for each RCHRES. BASINS, the user interface that accompanies the HSPF code, generates FTABLEs from a simplified reach file using preset channel geometry assumptions. Some assumptions of the channel geometry include a trapezoidal-shaped channel cross-section, channel sides with slopes of a 1:1 ratio, the flood plain width on each side of the reach being equal to the mean channel width, and the maximum depth in the FTABLE being 100 times the depth of the floodplain slope break [29].

One of the main problems with this simplified approach is that the BASINS-generated FTABLEs tend to have very few points within the range of the vast majority of actual flows. For example, in most of the HRUs there are only one to two data points in the BASINS-generated FTABLE that fall within all daily values for discharge. It is essential to develop FTABLEs that accurately reflect the major hydrological processes and water quality constituents such as sediment in order to ensure a realistic and unique simulation of the Sacramento River Basin. To enable a better simulation of suspended sediment, BASINS-generated FTABLEs were not used in the model; instead, FTABLEs were developed using hydraulic geometry. The heterogeneity of the Sacramento River watershed required two methodologies to develop FTABLEs; hydraulic geometry relationships were developed for the upland HRUs, and a one-dimensional hydraulic model was used for the lowland HRUs with very little slope.

#### Hydraulic Geometry Method

Regional hydraulic geometry relationships are often used to estimate channel dimensions for hydrologic models which require channel geometry data. Streamflow data from the National Water Information System (NWIS; [www.waterdata.usgs.gov](http://www.waterdata.usgs.gov)) contains channel dimension measurements including the width, depth, and watershed size. These measurements were used to develop FTABLEs by ranking each gage by calculated discharge frequencies over a range of discharge exceedances. Analyses were limited to 45 out of the 288 gages that had greater than 10 years of data, had not moved or changed significantly during the period of record, and had less than 5% missing data. For each of the 45 gages, field measurements of channel width, depth, and velocity over a range of streamflows were converted to at-a-station hydraulic geometry parameters using a power-law fit for width, depth, and velocity with discharge:

$$w = a \times Q^b \quad (1)$$

$$d = c \times Q^f \quad (2)$$

$$v = k \times Q^m \quad (3)$$

where  $w$  is the width (meters),  $d$  is the depth (meters),  $v$  is the velocity (meters per second),  $Q$  is the discharge (cubic meters per second) and  $a, b, c, f, k$ , and  $m$  are the power-law fit parameters [30].

The station power-law fit parameters (at-a-station) were scaled by each exceedance discharge (ranging from 0% to 100% of the maximum discharge). The power-law parameters for each exceedance discharge were then used to calculate the downstream hydraulic geometry [30]. For example, at the 50% exceedance discharge for width, the at-a-station power-law fit was used to estimate the width for all of the gages that were used to calculate a single power-law fit for the downstream hydraulic geometry for the width at the 50% exceedance flow ( $R^2 = 0.97$ ). Gages with zero discharge up to relatively high exceedances were removed because they violate the assumptions of the power law. Major reach segments (greater than a 10 km<sup>2</sup> drainage area and 10 km in length) were identified using GIS. Discharge was related to the drainage area for each gage and exceedance flow using a linear regression ( $R^2 = 0.93$ – $0.97$ ) (Figure 3) because discharge was not known for the majority of reaches in the model domain.

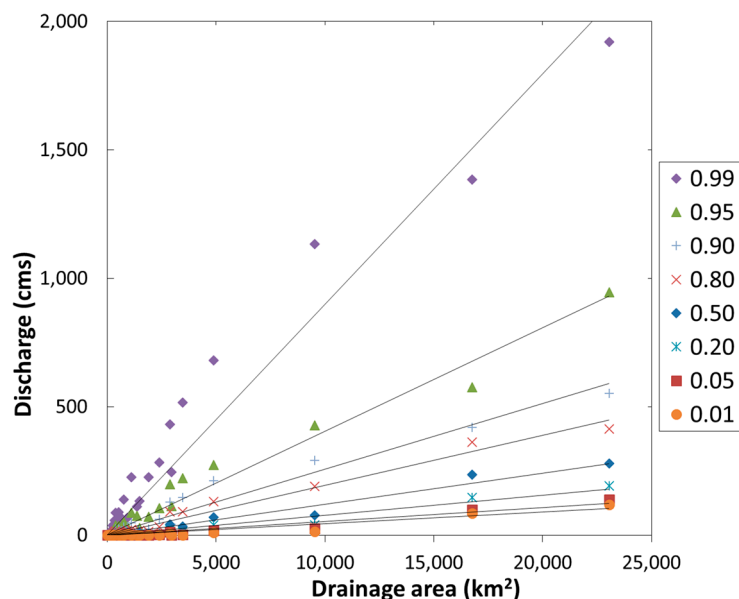


**Figure 3.** Discharge to drainage area relationship for stream gages within the model domain, grouped by exceedance discharge.

The hydraulic geometry was calculated for each reach and exceedance discharge using the drainage area-to-discharge regression equations and the downstream hydraulic geometry relationship. Each HRU contains multiple reaches that were represented in the model as a single RCHRES; therefore, the reach segments were summed to generate the final FTABLE assigned to the RCHRES. Several reaches on the Sacramento River include flood structures called weirs. The weirs included in the HSPF model are located on reaches 61, 98, 99, 90 and 97 (Figure 1). Adjustments were made to the FTABLES to enable observed changes in streamflow routing during high flows. At certain high flow levels, the simulated weir will divert water and sediment to an adjacent bypass.

### One-Dimensional Hydraulic Model Method

For seven of the lower-elevation HRUs in the valley floor (68, 78, 90, 94, 97, 98, 99), the hydraulic geometry method was not successful in formulating the FTABLES. The breakdown of the hydraulic geometry method was primarily due to the low elevational gradients and large flood plains. For these lowland HRUs, the Digital Elevation Model (DEM)-derived drainage routing and watershed area frequently did not follow known river channels because out-of-levee floodplain areas are routinely near or below the river water level, and the steepest descent path did not accurately follow the river channels.

Instead of using the hydraulic geometry method for these low-elevation, low-gradient HRUs, an existing one-dimensional (1-D) hydraulic model was used to create the FTABLES. The 1-D hydraulic model was created by the California Department of Water Resources (DWR) as part of the Central Valley Floodplain Evaluation and Delineation Program (CVFED) for the Sacramento River and its tributaries, with bathymetry and topography collected from 2001 to 2011 [31]. The CVFED hydraulic model was run with flow only within the major tributary channels (no flows overtopped the levees). The hydrologic inputs to the model were the same as those used for generating the aforementioned hydraulic geometry FTABLES. The FTABLES were created from the 1-D hydraulic model by calculating the channel surface area, depth and volume for each reach over a range of streamflows.

### 3. Calibration

The HSPF model calibration was done in three steps; snow was calibrated first, followed by hydrology and finally sediment. Standard calibration techniques were used to develop snow (S4),



and to develop initial hydraulic parameters (S5). Novel or non-standard calibration techniques are described below.

### 3.1. Hydrologic and Sediment Calibration

The HSPF model was calibrated for the period 1998–2008. The calibration period was chosen to include the land use data from 2006 and a wide range of annual precipitation. The calibration period included four wet years, one above-normal year, two below-normal years, three dry years, and one critically dry year [32]. Calibration runs were the initial test of the model, and using only data from 1998 to 2008, the parameters were changed iteratively to find an acceptable fit of modeled to observed data. Validation of the model was performed by calculating the goodness-of-fit statistics using a period of record other than what was used for model calibration. A successful model validation is indicated by the goodness-of-fit statistics being comparable to the results obtained for model calibration. The validation was completed using data only within the period 1980–1995. The validation period included five wet years, two above-normal years, four dry years and five critically dry years [32].

Hydrologic parameters were developed for all HRUs using spatially distributed physical properties to maintain a more accurate spatial representation of the model parameters in locations without calibration data. For example, infiltration capacity (INFILT) is one of the parameters to which modeled streamflow is the most sensitive [33], and initial values were assigned based on a spatially distributed map of the hydrologic soil group (HSG). Hydrologic soil groups range from “A” to “D”, where “A” soils are characterized by the highest infiltration rate and the lowest runoff potential and “D” soils have a very slow infiltration rate and the highest runoff potential. A range of values were scaled to the “typical” parameters listed in the BASINS Technical Note 6 (0.254–6.35) [34]. During the iterative process of calibration these values were raised or lowered in unison. Each hydrologic parameter was determined with this method using land use, soils data, and/or slope. There are “typical” and “possible” ranges for each parameter, although parameter values should reflect conditions in the watershed [34]. Every effort was made to derive parameter values that reflected the spatial characteristics of the watershed, even though they are lumped segments.

After the hydrologic calibration was complete, the sediment calibration was performed using a separate set of parameters related to sediment sources and transport capabilities in HRUs and reaches. Initial sediment parameters were based on GIS layers of soil properties, land use, and slope. The same iterative technique used to calibrate the hydrology was used to calibrate the sediment. Daily modeled sediment loads (tons/day) and suspended sediment concentrations (mg/L) were compared to observed data at NWIS gage locations with sediment data (Table S1).

### 3.2. Model Performance Evaluation

Goodness-of-fit statistics were calculated to quantitatively compare modeled and observed streamflow at stream gages selected for calibration and validation (Table S1). Three main statistical methods were used to assess the goodness-of-fit of the model results: the coefficient of determination ( $R^2$ ), the Nash-Sutcliffe coefficient of efficiency (NSE) [35], and mean error percent (ME%). The coefficient of determination ( $R^2$ ) is the square of the Pearson’s product-moment correlation coefficient ( $R$ ) and ranges from 0 to 1, with higher values indicating better agreement between modeled and observed data [36]. The NSE is the ratio of one minus the mean square error to the variance and is a widely used and reliable statistic for determining the goodness-of-fit for hydrologic models.

A value of 1 for NSE indicates a perfect match between observed and modeled data; values equal to zero indicate that the model is predicting no better than using the average of the observed data. Values less than zero indicate that the model does not do as good as the sample mean in predicting the observed values, and therefore indicates a poor model. NSE and  $R^2$  are sensitive to the extreme values [36]. A mean error (ME%) value closest to zero indicates a better simulation result. Hydrologic calibration results for the 20 gages were assessed for daily and monthly flows using the four statistical methods. The “model performance” is related to guidelines outlined by Donigan [37] (Table 1).

**Table 1.** Performance rating guidelines for daily and monthly flow statistics [37].  $R^2$  = coefficient of determination; ME% = mean error; NSE = Nash Sutcliffe efficiency.

Performance Rating	NSE		$R^2$		ME%	
	Daily	Monthly	Daily	Monthly	Daily	Monthly
Excellent	$\geq 0.85$	$\geq 0.90$	$\geq 0.85$	$\geq 0.90$	$\leq \pm 10$	$\leq \pm 5$
Very good	0.75–0.85	0.80–0.90	0.75–0.85	0.80–0.90	$\pm 10$ – $\pm 15$	$\pm 5$ – $\pm 10$
Good	0.65–0.75	0.70–0.80	0.65–0.75	0.70–0.80	$\pm 15$ – $\pm 25$	$\pm 10$ – $\pm 15$
Fair	0.50–0.65	0.50–0.70	0.50–0.65	0.50–0.70	$\pm 25$ – $\pm 30$	$\pm 15$ – $\pm 25$
Poor	$< 0.50$	$< 0.50$	$< 0.50$	$< 0.50$	$\geq \pm 30$	$\geq \pm 25$

## 4. Results

### 4.1. Hydrology Calibration Results

Qualitative comparisons of modeled to observed data were performed using hydrographs and flow-duration curves. Visual inspection of flow hydrographs for the calibration (Figure 4) and validation (Figure S2) periods showed a good relationship of modeled to observed data. The modeled summer low-flows tend to be higher than the observed data, and some of the smaller peak flows are underestimated. The highest modeled peaks generally correlated well with observed data but are overestimated in some cases.

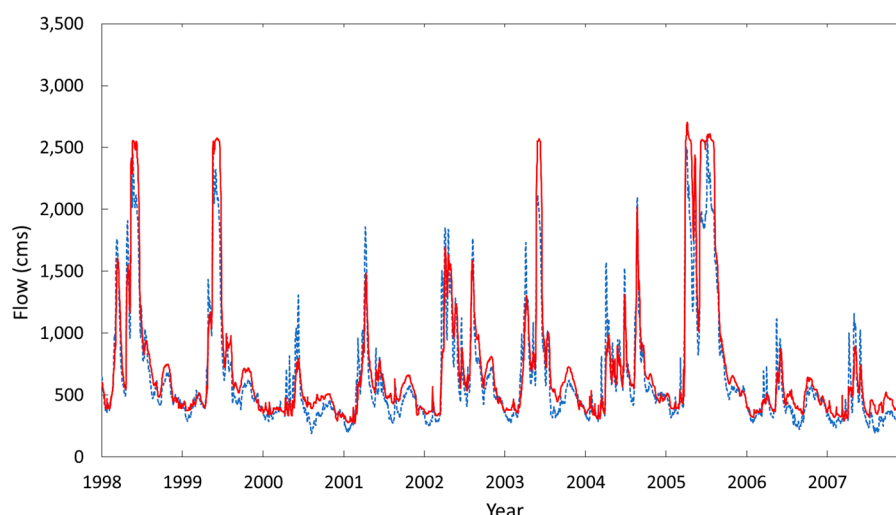


**Figure 4.** Modeled daily flow at reach 97 (Figure 1, solid red) compared to observed flow for Sacramento River at Freeport (11447650) (dashed blue) for the calibration period (1998–2008).

Flow-duration curves were also compared to ensure the realistic replication of hydrologic processes, with an emphasis on the higher flow regimes that typically move more sediment through the system. The flow-duration curves for the Sacramento River show that the overall relationship is similar to the observed flow, although the modeled flows tend to be higher than those observed and there is a divergence between the 2%–10% exceeded range likely due to how weirs are simulated in the model. The average  $R^2$  values for all reaches were 0.79 for daily flows and 0.91 for monthly flows for the entire simulation period (Table 2). The average  $R^2$  values for the Sacramento River during the entire simulation period were 0.92 and 0.96 for daily and monthly flows, respectively. The calibration process focused on achieving the best results for the Sacramento River rather than the contributing tributaries, because the objective of the study was to project potential future suspended sediment being discharged by the Sacramento River to the Bay-Delta, and therefore model accuracy was most critical for simulated flows of the Sacramento River. Calibration results indicated performance ratings

of “Very good” to “Excellent” for the Sacramento River gages using three statistical metrics used to evaluate the HSPF model (Table 2).

**Table 2.** Daily and monthly flow statistics for the simulation period, and the calibration and validation periods. Values are averages of all reaches or Sacramento River reaches only.  $R^2$  = coefficient of determination; ME% = mean error; NSE = Nash Sutcliffe efficiency.

Model Simulation Time Period		NSE		$R^2$		ME%	
		All Reaches <sup>1</sup>	Sacramento River	All Reaches <sup>1</sup>	Sacramento River	All Reaches <sup>1</sup>	Sacramento River
Simulation (1958–2008)	daily	0.69	0.90	0.79	0.92	−3%	−7%
	monthly	0.86	0.93	0.91	0.96	−7%	−7%
Calibration (1998–2008)	daily	0.70	0.89	0.74	0.92	20%	−10%
	monthly	0.78	0.92	0.84	0.96	11%	−10%
Validation (1980–1995)	daily	0.66	0.91	0.75	0.93	−15%	−11%
	monthly	0.83	0.94	0.88	0.97	−15%	−11%

Note: <sup>1</sup> Not including gages located on a bypass (Reaches 62, 78, and 94).

Full statistics for each gage show the variability of statistical results between gages (Table S4). Gages located on a bypass (62, 78, and 94) displayed high  $R^2$  values but also extremely high mean error percent values which were not included in the average statistics (Table 2). The combination of high mean error percent values with high correlation values was likely due to the bypasses not being explicitly modeled in HSPF, where modeled flow did not accurately represent the observed low flow recession and conversely overestimated high peaks compared to the observed data. Calibration focused on the Sacramento River reaches and the average statistics ranged from “Very good” to “Excellent”; the tributaries ranged from “Fair” to “Very good”, except for reaches with bypasses (Table 2 and Table S5). Monthly flow statistics were generally better than daily statistics, as shown in Table 2. Annual modeled streamflow at Sacramento River at Freeport generally matched well against observed data (Figure S3). The annual modeled peaks were slightly higher than observed data but were similar to the overall long-term trend. The regression lines for both data sets indicate a slight increasing trend but are not significant.

#### 4.2. Sediment Calibration Results

Modeled suspended sediment and total sediment loads were compared to annual sediment loads and daily suspended sediment concentrations and sediment loads from NWIS stream gages that contained historical sediment time series. Daily statistics ranged considerably (Table S5), and the calibration with emphasis on the Sacramento River resulted in higher  $R^2$  values and mean errors closer to zero for the Sacramento River gages. The modeled ratios divided by the observed ratios ranged considerably, but on average for all gages were 0.95 for sediment loads and 1.0 for SSC (Table 4). Sediment statistics were generally poorer than the hydrologic statistics because sediment transport is simulated using model components and assumptions associated with a higher degree of uncertainty, and this uncertainty is added to the uncertainty in the modeled flow values. Calibration focused on the Sacramento River resulted in a good calibration for daily and monthly sediment loads and SSC (Table 3).

The average daily  $R^2$  for sediment loads (for all gages) was 0.49 and the average  $R^2$  value for SSC was 0.38 (Table 3). Annual modeled sediment loads were compared for all gages on the Sacramento River with available sediment data (Table S1). Sediment outputs were converted to million metric tons (Mt) by water year (Figure 5). The relationship between modeled and observed annual sediment loads on the Sacramento River is nearly one to one, with an  $R^2$  of 0.81. The ratio of modeled to observed sediment loads is on average 1.12, with a mean error of 4%.

**Table 3.** Daily and monthly sediment statistics. Values are averages of all reaches or Sacramento River reaches only. SSC = suspended sediment concentrations;  $R^2$  = coefficient of determination; ME% = mean error.

SSC (mg/L) or Sediment Loads (Tons/Day)		Modeled/Observed		$R^2$		ME%	
		All Reaches	Sacramento River	All Reaches	Sacramento River	All Reaches	Sacramento River
Sediment loads	daily	0.95	0.89	0.49	0.52	400%	21%
	monthly	0.97	0.91	0.72	0.74	3131%	−9%
SSC	daily	1.0	0.92	0.38	0.37	486%	55%
	monthly	1.0	0.95	0.64	0.56	202%	23%

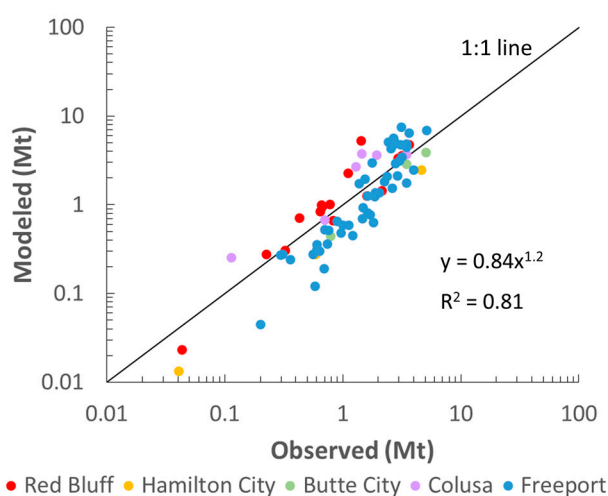


**Figure 5.** Comparison of modeled and observed annual sediment loads (million metric tons, Mt) for the gage locations Sacramento River at Red Bluff (1959–1970, 1977–1980), Hamilton City (1977–1979), Butte City (1978–1980), Colusa (1973, 1975, 1977–1980), and Freeport (1959–2008).

The annual modeled sediment loads for the Sacramento River at the Freeport gage reproduced the general measured trends (Figure S4) to use for the final calibration goal of demonstrating the long-term trends of sediment transport. Although the comparisons of individual water years are variable, the overall trend of modeled sediment over the past 50 years was similar to the measured data (Figure S4). There was more variability in the modeled data compared to the observed data on a year-to-year basis. The modeled annual SSC also showed a similar trend to the observed data, although there was significantly less variability in the modeled SSC data than with modeled sediment loads. Generally, modeled annual SSC slightly under-predicted observed SSC.

#### 4.3. Historical Trends in Streamflow and Sediment

Near the confluence of the Sacramento River and the Bay-Delta, there is a notable observed decrease in suspended sediment concentrations (SSC) in the past 50 years (1957–2001) [4]. One objective of this model was to calibrate to post-dam sediment loads to determine if the observed declining trend could be replicated and if the mechanisms for the decline could be elucidated. The current conceptual model describing the mechanisms and processes contributing to the sediment supply to the Bay-Delta suggest that human activities that alter watershed sediment supply are likely to have a greater effect on the river supply to the Bay-Delta than those that modify the flow regime [6]. Thus, they propose that the decline in SSC over the past 50 years was only moderately influenced by the climate. We intend to address the influence of the climate on the historical patterns of sediment transport. Historical flow



and sediment trends were assessed by dividing the annual data into the top and bottom 50% flow regimes (Figure 6).

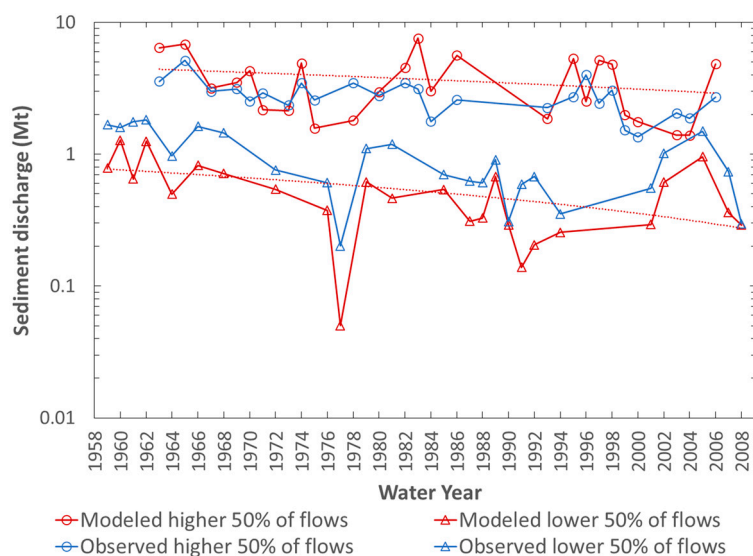


**Figure 6.** Comparison of modeled (red) and observed (blue) annual sediment loads (million metric tons, Mt) for the Sacramento River at Freeport gage. Flows are separated into highest and lowest 50% regimes.

Kendall's tau ( $\tau$ ) and Spearman's rho ( $\rho$ ) statistical tests were performed to determine the statistical significance and probability of monotonic time trends. At the Sacramento River at the Freeport gage location, there were no statistically significant trends in modeled annual streamflow for the model period (1958–2008). A statistically significant decreasing trend of annual sediment discharge over the 1958–2008 period was found at the Sacramento River at the Freeport gage in the lower 50% of flows ( $p = 0.01$ ,  $\rho$  and  $\tau$ ). There is also a slight decreasing trend in SSC for the lower 50% of annual flows, ( $p = 0.02$ ,  $\tau$ ).

Previous studies have examined suspended sediment trends from the greater Sacramento River Basin [4,16,38], though none have examined trends between the Sacramento River below Keswick to Verona (Figure 1) due to a lack of measured data. Statistically significant decreasing trends of modeled sediment were found at the Sacramento River at the Butte City gage (reach 49,  $p = 0.01$ ,  $0.02$   $\rho$  and  $\tau$ , respectively) and at the Sacramento River at the Colusa gage (reach 61,  $p = 0.03$ ,  $0.04$ ,  $\rho$  and  $\tau$ , respectively) for the lower 50% flow regime. Decreasing trends of varying magnitude were apparent at all of the gages on the Sacramento River, but were not statistically significant at the Red Bluff (reach 22) or Verona (reach 99) locations (Figure 1).

## 5. Historical Climate Trends

Although there was no significant mean annual change in flow or precipitation during the simulation period, simulated changes in the magnitude and frequency of precipitation, snow, and streamflow were analyzed to evaluate mechanisms that might lead to the decline of transported sediment. To determine the effects of climate change on streamflows, all inflows from dams and gages were removed to negate the influence of flow management from dams and diversions. The northern half of the model was located at the Sacramento River at the Butte City gage (BC) and the southern half of the model extended from BC to the Sacramento River at the Freeport gage (FPT). With no changes made to any spatially distributed properties over the simulation period, the 50-year simulation was divided into 1958–1983 and 1984–2008 to assess changes in flow solely related to climate. Suspended sediment transport was positively correlated to daily flow volumes with an  $R^2$  of greater than 0.9.

As the majority of sediment is transported by higher flows, peak precipitation days (>95%) were assessed, and these decreased by 8% and 10% at BC and FPT, respectively (Table 4).

**Table 4.** Precipitation, snow, and streamflow changes during the model simulation period (1958–2008). Units for precipitation and streamflow are number of peak days (>95%) and mm for snow.

Location	Variable	1958–1983	1984–2008	Percent Change
Sacramento River at Butte City	precipitation	476	438	−8%
	snow	26.2	23.8	−9%
	peak streamflow	487	427	−12%
Sacramento River at Freeport	precipitation	481	433	−10%
	snow	0.18	0.04	−76%
	peak streamflow	535	379	−29%

On average, the snow water equivalent decreased 9% for BC and 76% for FPT (Table 4). Peak streamflow days considering no model inflows declined 12% and 29% at BC and FPT, respectively (Table 4). Changes in timing were also observed at both BC and FPT. When the entire Sacramento Valley Basin is added together, it is clear from Figure 7 that the peak snow water equivalent occurs a month earlier in the second time period 1984–2008, and peak flows have declined in the three months of December through February. However, peak flows increased for the four months of March through June (Figure 7).

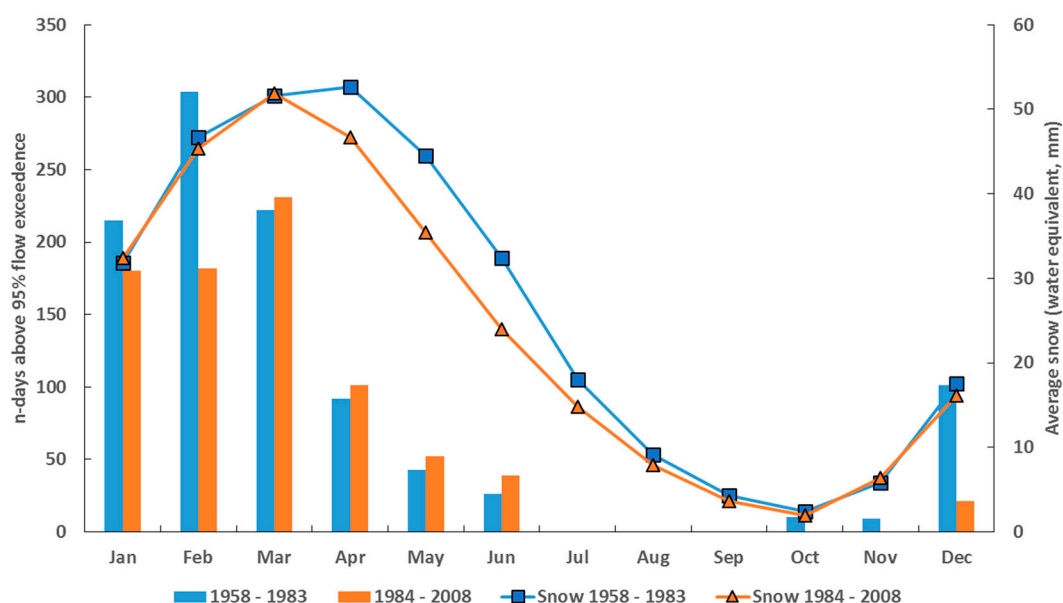


**Figure 7.** Modeled peak streamflow days (>95%) by month for the Sacramento River Basin with model inflows removed, for 1958–1983 (blue bars) and 1984–2008 (orange bars). Snow (water equivalent, mm) for the entire model domain is displayed on the right y-axis.

The mean temperature increased by 0.25 °C in the northern basin and 0.5 °C in the southern basin, contributing to the shift in snow accumulation and timing. The peak magnitude and frequency of precipitation and snow changed over the historical climate period, and thus peak streamflows were affected, although annual mean trends were not observed. The changes in the timing and magnitude of streamflows likely contributed to the observed decline in sediment transport for the Sacramento River Basin, thus providing more relative weight of the climate as a driver in the current conceptual model of sediment supply processes to the Bay-Delta [6].

## 6. Future Climate Sensitivity Analysis Using Climate Assessment Tool (CAT)

The model's sensitivity to future climate change was further explored by using the Climate Assessment Tool (CAT), a program within BASINS that provides capabilities for creating climate change scenarios using a calibrated HSPF model [39]. A wide range of "what if" questions about future weather and climate changes are possible to assess the effects on hydrology and water quality. The historical climate for 1958–2008 is considered the "base" period, and adjustments were made to precipitation, air temperature, and potential evapotranspiration to create possible "scenarios" of future climate. These scenarios were used to assess potential impacts and sensitivity to climate change on the hydrology and water quality for the Sacramento River Basin.

Several scenarios were developed to assess how sensitive hydrology and sediment transport are to climate change. While these hypothetical scenarios are useful to determine sensitivity of the hydrologic system to climate change, they are not projections or predictions of future climate variables. The scenarios chosen reflect a consensus of simulations of air temperature and precipitation change for northern California over the next century [40]. Air temperature is expected to increase by 1.5 °C under the lower emissions B1 scenario in the less conservative (in which greenhouse emissions are mitigated) climate model to an increase of 4.5 °C in the higher emissions A2 scenario with a more conservative (greenhouse emissions increase) climate model [40]. Precipitation is projected to change only slightly [40], so positive and negative changes of 10% were used to determine the sensitivity of streamflow to precipitation changes. Some future climate scenarios predicted an increase in the magnitude and frequency of large storms [41–43]; therefore, an increase of 10% for the storm magnitude and frequency was used in two of the hypothetical scenarios. A 10% increase in storm magnitude and frequency is defined in this scenario as a 10% increase in frequency and magnitude of the top 10% of storms by volume in the historical record (1958–2008).

The scenarios T1 and T2 were increases of temperature only (1.5 °C and 4.5 °C, respectively). The P1–P3 scenarios increased or decreased precipitation without changes in temperature. Scenarios W1–W4 were combinations of temperature increases (1.5 °C and 4.5 °C) and a 10% increase in precipitation or a 10% increase in storm magnitude and frequency (Table 5). The D1 and D2 scenarios were defined as a 10% decrease in precipitation with increases in air temperature of 1.5 °C or 4.5 °C. Potential evapotranspiration was recalculated for each scenario using the Hamon (1961) method, which is based on air temperature and therefore may overestimate PET. The sensitivity analysis using CAT was designed to assess how the baseline model responds to general changes in climate. For these hypothetical scenarios, the Hamon method was used because resources did not permit the recalculation of PET using the Priestley-Taylor method.

The baseline data were most sensitive to an increase of storm magnitude and frequency of 10% and no temperature change, where mean streamflow increased by 2.6%, sediment discharge increased by 9%, and SSC increased by 3.3%. Scenarios that included increases in temperature resulted in a decrease of streamflow, sediment discharge, and SSC, even scenarios with relatively large increases in precipitation. Streamflow and sediment displayed a slightly greater decline in response to a 10% increase of storm magnitude and frequency than an overall 10% increase in precipitation. Mean sediment discharge and SSC were more sensitive to changes in climate than mean streamflow. The most sensitive scenario which included a temperature change was D2, and resulted in decreases of 0.8% for streamflow, 7.9% for sediment discharge, and 8.5% for SSC (Table 5). Streamflow, sediment discharge, and SSC increased under most precipitation scenarios but began to decline at precipitation thresholds of −18%, −12%, and −19%, respectively. With increases of both temperature and precipitation, temperature had a stronger influence and therefore decreases were only seen in the T, W, and D scenarios. In the W and D scenarios, increases of the temperature from 1.5 °C to 4.5 °C only decreased streamflow and sediment by less than a percent.

**Table 5.** Hypothetical climate change scenarios generated using the Climate Assessment Tool (CAT). “BASE” scenario is the historical modeled flow for Reach 97 with units expressed in parentheses. Values for scenario results are expressed as a percent higher or lower than the base scenario. cms = cubic meters per second; SSC = suspended sediment concentration.

Scenario	Description	Mean Annual Streamflow (cms)	Mean Annual Sediment Discharge (Tons/Day)	Mean SSC (mg/L)
BASE	Reach 97 (1980–2008)	727	8604	41.5
		Change in Mean Streamflow (Percent)	Change in Mean Sediment Discharge (Percent)	Change in Mean SSC (Percent)
T1	Temperature +1.5 °C	−0.5	−7.7	−7.9
T2	Temperature +4.5 °C	−0.7	−7.9	−8.3
P1	Precipitation −10%	+0.5	+0.5	+0.6
P2	Precipitation +10%	+1.9	+5.1	+2.2
P3	Storm magnitude and frequency +10%	+2.6	+9.0	+3.3
W1	Temperature +1.5 °C, precipitation +10%	−0.5	−7.6	−7.9
W2	Temperature +4.5 °C, precipitation +10%	−0.6	−7.8	−8.2
W3	Temperature +1.5 °C, storm magnitude and frequency +10%	−0.6	−7.7	−8.0
W4	Temperature +4.5 °C, storm magnitude and frequency +10%	−0.7	−7.9	−8.4
D1	Temperature +1.5 °C, precipitation −10%	−0.7	−7.8	−8.1
D2	Temperature +4.5 °C, precipitation −10%	−0.8	−7.9	−8.5

## 7. Discussion

The main objective of this study was to characterize the hydrology and sediment transport in the Sacramento River Basin. The results provide streamflow and sediment boundary conditions to a hydrodynamic model of the Bay-Delta used to help project potential impacts to the hydrologic and ecological health of the Bay-Delta in response to climate change and variability. Spatial interpolation of meteorological data and the estimation of channel characteristics using hydraulic geometry modeling were used to develop model inputs that included many subdrainages and tributaries with sparse data. The parameterization techniques incorporated known spatial information for tributaries such as soils information, slope, and land cover. As part of the model calibration, parameters were adjusted uniformly using linear scaling to increase or decrease values in order to retain the spatial distribution of the physical characteristics of the land surface in un-gaged areas.

The hydrological calibration of the Sacramento Valley HSPF model provided statistical results for streamflow that showed a range of model accuracy for tributaries but the goodness-of-fit statistics for both calibration and validation for locations on the main branch of the Sacramento River ranged from “very good” to “excellent”. Sediment calibration also resulted in a wide range of accuracy depending on location, although simulation results at gages located on the Sacramento River averaged 11% higher than observed sediment loads and 8% higher than observed SSC. Based on statistical guidelines, the calibration of flow and sediment was very successful for the Sacramento River, owing in large part to the rigorous development of spatially distributed climate, the parameterization of physical properties, and extensive development of FTABLEs.

An important objective of this model was to calibrate to post-dam sediment loads in the Sacramento River Basin to determine if the observed declining trend could be replicated which has implications for the long-term sediment yield to the San Francisco Bay-Delta. A slight but statistically



significant decreasing trend was evident in the modeled suspended sediment and SSC results at the Sacramento River at the Freeport location from 1958 to 2008 in the lower 50% flow regime. No changes were made to hydrology or sediment parameters over the simulation time; therefore, changes in sediment must be attributed to managed inflows or climate. Although there was no overall change in flow over the model period, changes in timing and frequency of high flows due to warming and declining snow were observed and likely decreased the sediment yield over time.

The calibrated HSPF model was used to help evaluate the potential response of streamflow, sediment loads, and SSC to future climate change and variability using hypothetical climate scenarios. The base hydrology was most sensitive to an increase of the storm magnitude and frequency, with no temperature change. Snowpack losses are projected to increase through the next century [40], which will decrease snow pack accumulation and can cause a shift in the hydrologic timing: snow will melt earlier in spring, leaving less water during the summer months. A shift in the hydrologic timing of the peak streamflow was observed at the Butte City and Freeport locations. A significant decrease in the snow pack for the basin could explain the decrease and shift in timing of peak flows over the historical period at Butte City and Freeport. This change in hydrologic extremes and timing is likely a major driver in the decline in sediment at Freeport, since modeled sediment was more sensitive to changes in precipitation intensity than an average increase over time.

#### *Model Uncertainty*

Often the biggest measure of input uncertainty into HSPF is attributed to a scarcity of long-term climate stations as well as the quantity of stations available. The improvement of meteorological data and hydraulic function tables (FTABLEs) as well as the spatial distribution of physical properties are measures designed to reduce the amount of input-induced error into the model and rely more heavily on distributed processes to which the calibration parameters are physically related.

HSPF is a one-dimensional flow and transport model, and as such has known limitations for simulating river bank erosion, channel armoring, or longitudinal bed sediment movement. The Sacramento River is a gently sloping, meandering river with bed loads comprised predominantly of sand and gravel; therefore, the bed load contributions downstream and consequently to the Bay-Delta are minimal, and it was thus assumed that model limitations regarding more complex flow and transport processes had a minimal effect on the results in this location. In addition, many of the large tributaries below dams have experienced channel armoring, or the removal of finer sediment fractions from the bed. Therefore, bed loads in this model domain were assumed to contribute a minimal amount to the total modeled sediment loads.

HSPF is a semi-lumped model, which causes inherent error due to the assumption that each sub-watershed is physically homogeneous. In addition, the model can only process a certain number of operations (model segments and hydrologic reach segments), creating the need for larger HRUs within the model domain and, in this case, two sub-models. Considering the complexity and size of the model, uncertainty is a concern and can come from the lack of diversion data from water transfers, agricultural uses, return flows, and the pumping of groundwater, which were not explicitly modeled. Calibration results for simulated versus observed snow accumulation and melting indicated that model uncertainty might be reduced if a more detailed discretization of HRUs (smaller HRUs) was applied to the higher-elevation subdrainages to better represent orographic effects on air temperature and precipitation. The lack of long-term sediment data and accumulation or erosion information within the domain led to uncertainties of the interpretation of areas that could be either a sediment sink or source. Input data, model or user assumptions, and parameter uncertainty can also introduce errors in modeling on such a large scale.

## **8. Conclusions**

The development of well-calibrated, spatially distributed, mechanistic models, such as this one of the Sacramento Valley below major dams, provides a valuable tool to characterize the mechanisms and

climatic signals that are responsible for flow and transport in a large basin. While there are limitations to the parameterization of these models, when all parameters are held constant over time, the changes in climate and how they influence flow and transport can be scrutinized. Unique parameterization of this basin helps identify where more data is needed to further understand physical processes that affect sediment transport. The ability to isolate land use change and water management provided the opportunity to evaluate historical changes as well as potential future changes in climate. In this watershed, the changes in the historical climate, with warmer temperatures and declines in snowpack, result in fewer peak flows, which translate into a meaningful and significant mechanism responsible for the long-term declining trend in sediment transport to complement the existing conceptual model [6] that relies on anthropogenic drivers such as historical land use change and water management. This conceptual model suggests that climate has only a moderate influence on sediment transport and plays no role in the historical decline of sediment to the Bay-Delta. In contrast, our analyses of historical climate in conjunction with sensitivity analyses support an increase in the role of climate on transport, particularly the role of large storms that result in high peak flows. As a result of diminishing snowpack over the last 50 years, and the likelihood of this continuing trend with global warming, the role of climate should be emphasized alongside anthropogenic influences in sediment transport to the Bay-Delta. Simulated future trends of sediment transport in the Sacramento River basin and understanding the mechanisms behind the trends are imperative to projecting the future health of the Bay-Delta ecosystem.

For the CASCaDE II project, future climate scenarios will be used to make projections of projected hydrologic and sediment trends during the period 2010–2100. The HSPF model will provide a direct coupling of the current and future climate with the potential sediment sources to estimate sediment supply to the Bay-Delta. Outputs from this model will be used as sediment boundary conditions for a hydrodynamic model to assess the future of the San Francisco Bay-Delta estuary-watershed system under the cascading effects of Delta configurational changes and climate change.

**Supplementary Materials:** The following are available online at [www.mdpi.com/2073-4441/8/10/432/s1](http://www.mdpi.com/2073-4441/8/10/432/s1).

**Acknowledgments:** This project was supported by the Computational Assessments of Scenarios of Change for the Delta Ecosystem (CASCaDE II) project. CASCaDE II is supported by a grant from the Delta Science Program (DSC Grant #2040). Any opinions, findings, and conclusions or recommendations expressed in this material are those of the authors and do not necessarily reflect the views of the Delta Science Program. This is CASCaDE publication #71.

**Author Contributions:** Lorraine Flint and Scott Wright conceived and designed the experiments; Michelle Stern performed the modeling and data collection; Michelle Stern, Lorraine Flint, Justin Minear and Scott Wright analyzed the data; Lorraine Flint, Alan Flint, Justin Minear and Scott Wright contributed inputs to the model; Michelle Stern and Lorraine Flint wrote the paper.

**Conflicts of Interest:** The authors declare no conflict of interest. The founding sponsors had no role in the design of the study; in the collection, analyses, or interpretation of data; in the writing of the manuscript, and in the decision to publish the results.

## Abbreviations

The following abbreviations are used in this manuscript:

BASINS	Better Assessment Science Integrating Point and Nonpoint Sources program
CAT	Climate Assessment Tool
CDEC	California Data Exchange Center
CIMIS	California Irrigation Management Information System
CVFED	Central Valley Floodplain Evaluation and Delineation Program
DEM	Digital Elevation Model
DWR	California Department of Water Resources
FTABLE	Hydraulic Function Table
GIDS	Gradient Inverse Distance Squared Interpolation
GIS	Geographic Information System
HSPF	Hydrological Simulation Program: FORTRAN
HRU	hydrologic response unit
HSG	Hydrologic Soil Group

HUC	USGS Hydrologic Unit (watershed) code
IMPLND	Impervious Land Segment
INFILT	Index to the Infiltration Capacity of the Soil
km	Kilometer
m	Meter
mm	Millimeter
ME%	Mean error percent
mg/L	Milligrams per liter
Mt	Million metric tons
NED	National Elevation Dataset
NHD	National Hydrography Dataset
NID	National Inventory of Dams
NLCD	National Land Cover Dataset
NSE	Nash Sutcliffe coefficient of efficiency
NWIS	National Water Information System
PERLND	Pervious Land Segment
PET	Potential Evapotranspiration
PRISM	Parameter-elevation Regressions on Independent Slopes Model
R	Correlation Coefficient
R <sup>2</sup>	Coefficient of Determination
RCHRES	Modeled Reach or Reservoir
SSC	suspended sediment concentration
SSURGO	Soil Survey Geographic Database
SWE	snow water equivalent
UCI	user control input file
USGS	United States Geological Survey
WY	water year

## References

1. Interagency Ecological Program (IEP). Dayflow. 2005; Available online: <http://iep.water.ca.gov/dayflow/index.html> (accessed on 3 February 2014).
2. CASCaDE: Computational A of Scenarios of Change for the Delta Ecosystem. Available online: <http://cascade.wr.usgs.gov> (accessed on 4 April 2016).
3. Ganju, N.K.; Schoellhamer, D.H. Decadal-timescale estuarine geomorphic change under future scenarios of climate and sediment supply. *Estuar. Coasts* **2010**, *33*, 15–29. [[CrossRef](#)]
4. Wright, S.A.; Schoellhamer, D.H. Trends in the sediment yield of the Sacramento River, California, 1957–2001. *San Franc. Estuary Watershed Sci.* **2004**, *2*, 1–14.
5. Cloern, J.E.; Knowles, N.; Brown, L.R.; Cayan, D.R.; Dettinger, M.D.; Morgan, T.L.; Schoellhamer, D.H.; Stacey, M.T.; van der Wegen, M.; Wagner, R.W.; et al. Projected Evolution of California's San Francisco Bay-Delta River System in a Century of Climate Change. *PLoS ONE* **2011**, *6*, e24465. [[CrossRef](#)] [[PubMed](#)]
6. Schoellhamer, D.H.; Wright, S.A.; Drexler, J. A Conceptual model of sedimentation in the Sacramento-San Joaquin Delta. *San Franc. Estuary Watershed Sci.* **2012**, *10*, 1–25.
7. Singer, M.B.; Dunne, T. An empirical-stochastic, event-based program for simulating inflow from a tributary network: Framework and application to the Sacramento River basin, California. *Water Resour. Res.* **2004**, *40*. [[CrossRef](#)]
8. Singer, M.B. The influence of major dams on hydrology through the drainage network of the Sacramento River Basin, California. *River Res. Appl.* **2007**, *23*, 55–72. [[CrossRef](#)]
9. California Department of Water Resources. California Water Plan Update 2013. Available online: [http://www.water.ca.gov/waterplan/docs/cwpu2013/Final/Vol2\\_SacramentoRiverRR.pdf](http://www.water.ca.gov/waterplan/docs/cwpu2013/Final/Vol2_SacramentoRiverRR.pdf) (accessed on 11 April 2016).
10. Bicknell, B.R.; Imhoff, J.C.; Kittle, J.L., Jr.; Donigian, A.S., Jr.; Johanson, R.C. *Hydrologic Simulation Program—FORTRAN, User's Manual for Version 12*; U.S. EPA Environmental Research Laboratory: Athens, GA, USA, 2001; pp. 1–755.
11. Donigian, A.S.; Bicknell, B.R.; Imhoff, J.C. Hydrological Simulation Program—FORTRAN (HSPF). In *Computer Models of Watershed Hydrology*; Singh, V.P., Ed.; Water Resources Publications: Highlands Ranch, CO, USA, 1995; pp. 395–442.

12. Fry, J.A.; Xian, G.; Jin, S.; Dewitz, J.A.; Homer, C.G.; Limin, Y.; Barnes, C.A.; Herold, N.D.; Wickham, J.D. Completion of the 2006 National Land Cover Database for the Conterminous United States. *Photogramm. Eng. Remote Sens.* **2011**, *77*, 858–864.
13. Gesch, D.; Evans, G.; Mauck, J.; Hutchinson, J.; Carswell, W.J. The national map—Elevation. *U.S. Geological Survey Fact Sheet 2009–3053*; U.S. Geological Survey: Reston, VA, USA, 2009; p. 4. Available online: <http://pubs.usgs.gov/fs/2009/3053/> (accessed on 5 September 2013).
14. Simley, J.; Carswell, W.J. *The National Map—Hydrography*; U.S. Geological Survey: Reston, VA USA, 2009; Volume 3054, p. 4.
15. Soil Survey Staff. Web Soil Survey. Available online: <http://websoilsurvey.nrcs.usda.gov/> (accessed on 5 September 2013).
16. Chen, C.W.; Herr, J.W. *Comparison of BASINS and WARME Models: Mica Creek Watershed*; Electric Power Research Institute: Palo Alto, CA, USA, 2002.
17. Nigro, J.; Toll, D.; Partington, E.; Ni-Meister, W.; Shihyan, L.; Gutierrez-Magness, A.; Engman, T.; Arsenault, K. NASA-modified precipitation products to improve USEPA nonpoint source water quality modeling for the Chesapeake Bay. *J. Environ. Qual.* **2010**, *39*, 1388–1401. [[PubMed](#)]
18. Laroche, A.M.; Gallichand, J.; Lagace, R.; Pesant, A. Simulating atrazine transport with HSPF in an agricultural watershed. *J. Environ. Eng.* **1996**, *122*, 622–630. [[CrossRef](#)]
19. Albek, M.; Ogutveren, U.B.; Albek, E. Hydrological modeling of Seydi Suyu watershed (Turkey) with HSPF. *J. Hydrol.* **2004**, *285*, 260–271. [[CrossRef](#)]
20. Kim, S.M.; Benham, B.L.; Brannan, K.M.; Zeckoski, R.W.; Doherty, J. Comparison of hydrologic calibration of HSPF using automatic and manual methods. *Water Resour. Res.* **2007**, *43*. [[CrossRef](#)]
21. Tong, S.T.Y.; Sun, Y.; Ranatunga, T.; He, J.; Yang, Y.J. Predicting plausible impacts of sets of climate and land use change scenarios on water resources. *Appl. Geogr.* **2012**, *32*, 477–489. [[CrossRef](#)]
22. Hayashi, S.; Murakami, S.; Watanabe, M.; Bao-Hua, X. HSPF simulation of runoff and sediment loads in the Upper Changjiang River Basin, China. *J. Environ. Eng.* **2004**, *130*, 801–815. [[CrossRef](#)]
23. Nalder, I.A.; Wein, R.W. Spatial interpolation of climatic normals: Test of a new method in the Canadian boreal forest. *Agric. For. Meteorol.* **1998**, *92*, 211–225. [[CrossRef](#)]
24. Flint, L.E.; Flint, A.L. Downscaling future climate scenarios to fine scales for hydrologic and ecological modeling and analysis. *Ecol. Process.* **2012**, *1*, 1–15. [[CrossRef](#)]
25. Daly, C.; Halbleib, M.; Smith, J.I.; Gibson, W.P.; Doggett, M.K.; Taylor, G.H.; Curtis, J.; Pasteris, P.P. Physiographically-sensitive mapping of temperature and precipitation across the conterminous United States. *Int. J. Climatol.* **2008**, *28*, 2031–2064. [[CrossRef](#)]
26. Priestley, C.H.B.; Taylor, R.J. On the assessment of surface heat flux and evaporation using large-scale parameters. *Mon. Weather Rev.* **1972**, *100*, 81–92. [[CrossRef](#)]
27. Bristow, K.L.; Campbell, G.S. On the relationship between incoming solar radiation and daily maximum and minimum temperature. *Agric. For. Meteorol.* **1984**, *31*, 159–166. [[CrossRef](#)]
28. Milly, P.C.D.; Dunne, K.A. On the hydrologic adjustment of climate-model projections: The potential pitfall of potential evapotranspiration. *Earth Interact.* **2011**, *15*, 1–14. [[CrossRef](#)]
29. U.S. Environmental Protection Agency. *BASINS Technical Note 1: Creating Hydraulic Function Tables (FTABLES) for Reservoirs in BASINS*; Office of Water: Washington, DC, USA, 2007.
30. Leopold, L.B.; Maddock, T., Jr. *The Hydraulic Geometry of Stream Channels and Some Physiographic Implications*; U.S. Geological Survey Professional Paper 252; U.S. Geological Survey: Reston, VA, USA, 1953; pp. 1–57.
31. Gainey, J.; California Department of Water Resources. CVFED Program, Central Valley Floodplain Delineation. Personal communication, 25 February 2014.
32. CA DWR Water Supply Information. Available online: [http://cdec.water.ca.gov/water\\_supply.html](http://cdec.water.ca.gov/water_supply.html) (accessed on 25 April 2014).
33. Fonesca, A.; Ames, D.P.; Yang, P.; Botelho, C.; Boaventura, R.; Vilar, V. Watershed model parameter estimation and uncertainty in data-limited environments. *Environ. Model. Softw.* **2014**, *51*, 84–93. [[CrossRef](#)]
34. U.S. Environmental Protection Agency. *Estimating Hydrology and Hydraulic Parameters for HSPF: EPA BASINS Technical Note 6*; Office of Water: Washington, DC, USA, 2000; Volume 4305, p. 32.
35. Nash, J.E.; Sutcliffe, J.V. River flow forecasting through conceptual models, I, A discussion of principles. *J. Hydrol.* **1970**, *10*, 282–290. [[CrossRef](#)]



36. Legates, D.R.; McCabe, G.J. Evaluating the use of “goodness-of-fit” measures in hydrologic and hydroclimatic model validation. *Water Resour. Res.* **1999**, *35*, 233–241. [[CrossRef](#)]
37. Donigian, A.J. Watershed model calibration and validation: The HSPF experience. *Proc. Water Environ. Fed.* **2002**, *8*, 44–73. [[CrossRef](#)]
38. McKee, L.J.; Ganju, N.K.; Schoellhamer, D.H. Estimates of suspended sediment entering San Francisco Bay from the Sacramento and San Joaquin Delta, San Francisco Bay, California. *J. Hydrol.* **2006**, *323*, 335–352. [[CrossRef](#)]
39. U.S. Environmental Protection Agency. *BASINS 4.0 Climate Assessment Tool (CAT): Supporting Documentation and User’s Manual*; EPA/600/R-08/088F; EPA: Washington, DC, USA, 2009.
40. Cayan, D.R.; Maurer, E.P.; Dettinger, M.D.; Tyree, M.; Hayhoe, K. Climate change scenarios for the California region. *Clim. Chang.* **2008**, *87*, 21–42. [[CrossRef](#)]
41. Cayan, D.R.; Tyree, M.; Dettinger, M.D.; Hidalgo, H.; Das, T.; Maurer, E.; Bromirski, P.; Graham, N.; Flick, R. *Climate Change Scenarios and Sea Level Rise Estimates for California 2008 Climate Change Scenarios Assessment*; PIER Research Report, CEC-500-2009-014-D; California Climate Change Center: Sacramento, CA, USA, 2009.
42. Dettinger, M.D. Climate change, atmospheric rivers, and floods in California—A multimodel analysis of storm frequency and magnitude changes. *JAWRA* **2011**, *47*, 514–523. [[CrossRef](#)]
43. Trenberth, K.E. Conceptual framework for changes of extremes of the hydrological cycle with climate change. *Clim. Chang.* **1999**, *42*, 327–339. [[CrossRef](#)]



© 2016 by the authors; licensee MDPI, Basel, Switzerland. This article is an open access article distributed under the terms and conditions of the Creative Commons Attribution (CC-BY) license (<http://creativecommons.org/licenses/by/4.0/>).